Luminescence Resonance Energy Transfer Measurements in Myosin

Elise Burmeister Getz,*# Roger Cooke,# and Paul R. Selvin*§

*Life Sciences Division, Lawrence Berkeley National Laboratory, Berkeley, California 94720; #Department of Biochemistry and Biophysics and the Cardiovascular Research Institute, University of California, San Francisco, California 94143; §Department of Physics, University of Illinois, Urbana, Illinois 61801 USA

ABSTRACT Myosin is thought to generate force by a rotation between the relative orientations of two domains. Direct measurements of distances between the domains could potentially confirm and quantify these conformational changes, but efforts have been hampered by the large distances involved. Here we show that luminescence resonance energy transfer (LRET), which uses a luminescent lanthanide as the energy-transfer donor, is capable of measuring these long distances. Specifically, we measure distances between the catalytic domain (Cys^{707}) and regulatory light chain domain (Cys^{108}) of the myosin head. An energy transfer efficiency of 21.2 ± 1.9% is measured in the myosin complex without nucleotide or actin, corresponding to a distance of 73 Å, consistent with the crystal structure of Rayment et al. Upon binding to actin, the energy transfer efficiency decreases by 4.5 ± 1.0%, indicating a conformational change in myosin that involves a relative rotation and/or translation of Cys^{707} relative to the light chain domain. Addition of ADP also alters the energy transfer efficiency, likely through a rotation of the probe attached to Cys^{707}. These results demonstrate that LRET is capable of making accurate measurements on the relatively large actomyosin complex, and is capable of detecting conformational changes between the catalytic and light chain domains of myosin.

INTRODUCTION

The myosin head contains two distinct parts, the catalytic domain that binds to actin and hydrolyzes ATP, and the light chain domain that connects the catalytic domain to the rod. The catalytic domain is composed of the heavy chain, and the light chain domain is composed of an α-helix of the heavy chain bound by two light chains—the regulatory light chain (RLC) and the essential light chain. Conformational changes within the myosin head as it interacts with actin are believed to be responsible for force generation in muscle and for a variety of subcellular motions in eucaryotes (Huxley, 1965; Rayment et al., 1993b; Spudich, 1994).

The catalytic domain has been shown to attach rigidly to actin during the force-producing cycle (for a review see Cooke, 1997). The structure of the myosin head has thus suggested a model for force production in which the light chain domain rotates relative to the catalytic domain, causing a translation of the actin filament, the so-called powerstroke. In this "lever arm" model, rotation of the light chain domain amplifies nucleotide-mediated conformational changes in the catalytic domain. Specifically, the light chain domain is believed to undergo a rotation of ~45° during the powerstroke to produce a 5–11-nm translation of the actin filament (Finer et al., 1994). The detection of such conformational changes during and surrounding the powerstroke is central to an understanding of muscle mechanics and energetics.

Despite intensive efforts, direct detection of the conformational changes occurring during the powerstroke has yet to be achieved. Rayment et al. (1993b) have crystallized the myosin head in the absence of nucleotides, including light chains, and have crystallized the myosin head without light chains complexed to various nucleotide analogs, some of which are believed to simulate the prepowerstroke state (Fisher et al., 1995; Smith and Rayment, 1995, 1996). The crystal structure for myosin in the absence of nucleotide, which is believed to resemble the postpowerstroke state, has been docked to molecular models of F-actin, guided by low-resolution cryoelectron microscopic images of the actomyosin complex (Rayment et al., 1993a; Schröder et al., 1993). These efforts lend support to the lever arm model, but a lack of electron density in the light chain domain for the docked structure prohibits a definitive determination of the orientation between the light chain domain and the catalytic domain. The crystal structure of myosin obtained in the presence of nucleotides shows shifts in the positions of several specific secondary elements; however, because of a lack of light chains in these structures, these conformational changes have not been linked directly to changes in the orientation of the light chain domain. Low-angle x-ray and neutron scattering have detected a global conformational change in the radius of gyration of the myosin head, but the technique cannot isolate conformational changes to a particular domain (Mendelson et al., 1996; Wakabayshi et al., 1992).

Two recent investigations have provided the most definitive evidence for rotation of the myosin light chain domain during the powerstroke. Irving et al. detected a 3° rotation during rapid length changes of muscle fibers via fluorescence depolarization of a probe bound to the RLC (Irving et al., 1995). Baker et al., using electron paramagnetic resonance (EPR) probes attached to the light chains in scallop

Received for publication 24 March 1997 and in final form 27 January 1998.

Address reprint requests to Dr. Paul Selvin, Loomis Laboratory of Physics, 1110 W. Green St., University of Illinois, Urbana, IL 61801. Tel.: 217-244-3371; Fax: 217-244-7187; E-mail: selvin@uiuc.edu.

0006-3495/98/05/2451/08 $2.00

muscle fibers, detected two distinct angles of the light chain domain with different distributions among these populations, depending on the state of the fiber (Baker et al., in press). Two other groups have detected a light chain domain swing during what is believed to be a postpowerstroke motion. Jontes et al. (1995), using electron microscopy, and Gollub et al. (1996), using EPR spectroscopy, both detected a rotation of the light chain domain of ~30° in smooth muscle upon ADP release.

Most spectroscopic probes attached to the light chain domain, which are potentially sensitive to rotational motion, have not been able to detect rotational changes during steady state activity, in part because the light chain domain appears to be highly disordered in active muscle (Allen et al., 1996; Hambly et al., 1992). An alternative method of detecting a swing of the light chain domain that does not rely on rotational probes is to measure distances between the light chain and catalytic domains before and after the powerstroke via fluorescence resonance energy transfer (FRET) (dos Remedios et al., 1987; Smyczynski and Kasprzak, 1997), but the distances between the regulatory light chain and catalytic domains are generally beyond the technique's range.

We have previously shown in model systems that using luminescent lanthanides as donors and conventional organic dyes as acceptors in luminescence resonance energy transfer (LRET) measurements leads to many technical advantages over conventional FRET (Li and Selvin, 1997; Selvin, 1995, 1996; Selvin and Hearst, 1994; Selvin et al., 1994). (Lanthanide emission arises from high-spin to high-spin electronic transitions and so is formally not fluorescence, but Förster's dipole-dipole theory nevertheless applies, because the transitions are primarily electric dipole (see Selvin and Hearst, 1994, and Selvin, 1996, for a discussion).) Others have shown the advantages of using lanthanides in energy transfer-based homogeneous assays (Mathis, 1993, 1995), in diffusion-enhanced energy transfer studies (Stryer et al., 1982), and for distance determination in calcium-binding proteins (Horrocks et al., 1975). Recently LRET has been used to measure protein-DNA interactions (Heyduk et al., 1997) and protein-protein interactions (Root, 1997).

Here we apply LRET to actomyosin, measuring energy transfer between a lanthanide donor on the regulatory light chain and an acceptor in the catalytic domain. For our initial study presented here, we have labeled the catalytic domain at Cys^{707} because labeling is specific and well characterized. However, Cys^{707} is near the putative fulcrum (Uyeda et al., 1996), and hence these measurements may not be very sensitive to the hypothesized swing of the light chain domain. Nevertheless, we show that LRET measurements on purified heavy meromyosin (HMM) are capable of measuring the requisite distances between catalytic and light chain domains, that the measured distance in the absence of nucleotide is consistent with the crystal structure, and that myosin adopts a different conformation upon binding actin and actin plus ADP.

MATERIALS AND METHODS

Proteins and reagents

HMM and actin were isolated and purified from rabbit skeletal muscle by standard methods (Spudich and Watt, 1971; Weeds and Pope, 1977). Chicken gizzard regulatory light chain (RLC) was a gift of Dr. Christine Cremo. 5-Tetramethylrhodamine iodoacetamide (TMRIA) and tris-(2-carboxyethyl) phosphine hydrochloride (TCEP) were purchased from Molecular Probes (Eugene, OR), and anhydrous dimethylsulfoxide and terbium chloride hexahydrate (99.999%) were purchased from Aldrich. The synthesis of diethylenetriaminepentacetate-carbostyril 124–maleimidopropionic hydrazide (DTPA-cs124-EMPH) will be published elsewhere (see Fig. 1). Light chain exchange buffer contained 1 mM ADP, 50 mM KCl, 10 mM EDTA, 10 mM KH_2PO_4 (or 50 mM 3-(*N*-morpholino)propanesulfonic acid, MOPS), pH 7.0. Rigor buffer contained 1 mM EGTA, 5 mM $MgCl_2$, 20 mM MOPS, pH 7.0. TCEP (5 mM) was added to all buffers on the day of use.

ATPase assays

ATPase activities were measured by determining the rate of release of inorganic phosphate (P_i) at 25°C, with the method of Kodama et al. (1986). K^+-ATPase was assayed in 0.6 M KCl, 1 mM EDTA, 50 mM MOPS, pH 7.0. Ca^{2+}-ATPase was assayed in 0.6 M KCl, 4 mM $CaCl_2$, 50 mM MOPS, pH 7.0. Actin-activated Mg^{2+}-ATPase was assayed in 2 mM $MgCl_2$, 20 mM MOPS, pH 7.0, with 80 μM actin. The reaction was initiated by adding 2 mM ATP. At 20, 60, 120, 180, 240, and 300 s, aliquots were quenched with 3.1% perchloric acid. The rate of ATP hydrolysis was constant during this time.

Acceptor labeling

Labeling protocol

Mole ratios of TMRIA to HMM varying from 2:1 to 50:1 were reacted overnight on ice in rigor buffer (at both pH 6.5 and pH 7.0). HMM concentrations during labeling were ~15 μM. The reaction was quenched by the addition of 10 mM dithiothreitol (DTT), and passed over a G-75 Sephadex size-exclusion column to remove free TMRIA. The goal was to achieve 2 TMRIA/HMM, with one TMRIA at each Cys^{707} site on the HMM dimer. This degree of labeling was achieved by reacting mole ratios of TMRIA to HMM between 3 and 6.

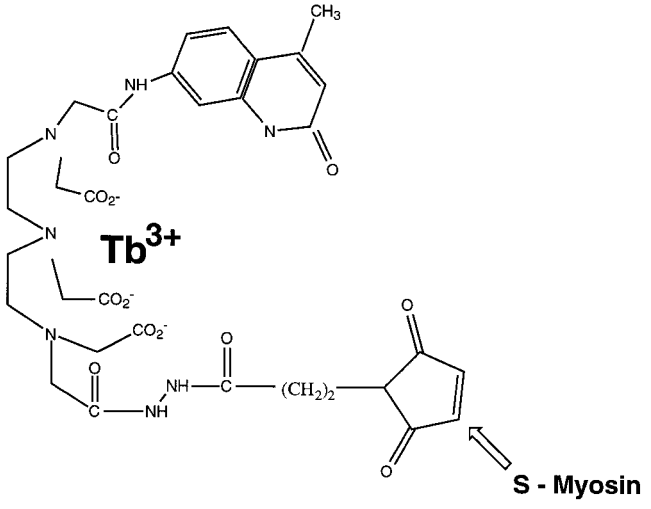

FIGURE 1 Structure of the terbium chelate (Tb-DTPA-cs124-EMPH) used as the energy transfer donor.

TMRIA extinction coefficient

The extinction coefficient of TMRIA bound to myosin was determined by measuring the absorbance of a known amount of TMRIA reacted with excess myosin and accounting for a small percentage of TMRIA that did not bind. Specifically, whole skeletal myosin (15 μM) was reacted with TMRIA (10 μM) on ice for 2 h in a buffer containing 0.6 M KCl, 5 mM $MgCl_2$, 20 mM MOPS, pH 6.5. At 0, 1, 5, 30, 60, and 120 min, the absorbance of this sample was measured, and the extinction coefficient (ϵ) was calculated according to: $\epsilon = (A_{554} - A_{650})/[\text{TMRIA}]$, where A_{554} and A_{650} are the absorbances at 554 nm and 650 nm, respectively (the latter to account for baseline offset). During the course of the 2-h reaction, the extinction coefficient of TMRIA decreased monotonically from 79 mM^{-1} cm^{-1} for free TMRIA, to 69 mM^{-1} cm^{-1} for TMRIA bound to myosin. In addition, to determine the extinction coefficient of sulfhydryl-reacted TMRIA at 280 nm and 330 nm, relative to the extinction coefficient at 554 nm (these values are used in determining the concentration of protein labeled with TMRIA), 10 μM TMRIA was reacted with 1 mM β-mercaptoethanol overnight. For this sample, A_{280}/A_{554} ($= \epsilon_{280}/\epsilon_{554}$) was 0.29, and A_{330}/A_{554} ($= \epsilon_{330}/\epsilon_{554}$) was 0.07.

Extent of TMRIA labeling

The extent of labeling and concentrations of HMM and bound TMRIA were determined by measuring the absorbance at 280 nm (primarily HMM absorbance, with some TMRIA absorbance), 330 nm (scattering and TMRIA absorbance), 554 nm (TMRIA absorbance), and 650 nm (baseline). The concentrations of HMM and TMRIA, in moles/liter, were then determined from Eqs. 1 and 2, respectively:

$$[\text{HMM}] = \{[(A_{280} - A_{650}) - 0.29(A_{554} - A_{650})] - 1.5[(A_{330} - A_{650}) - 0.07(A_{554} - A_{650})]\}/2.345 \times 10^5 \quad (1)$$

$$[\text{TMRIA}] = (A_{554} - A_{650})/69 \times 10^3 \quad (2)$$

For the HMM samples on which the LRET measurements were made, the extent of TMRIA bound per HMM head was determined to be 1.27 ± 0.09 ($n = 5$).

Location of TMRIA on HMM

The location of TMRIA on the protein was analyzed by tryptic digestion of the labeled HMM, followed by separation of the fragments by sodium dodecyl sulfate–polyacrylamide gel electrophoresis (SDS-PAGE). UV-induced fluorescence of the gel localized the TMRIA, followed by Coomassie blue staining, which gave a semi-quantitative measure of protein content in each band. For relatively light labeling (0.8–1.5 TMRIA bound per HMM head), no labeling of the endogenous RLC was detected, and the vast majority (~90%) of the fluorescence arose from a 20-kDa fragment known to contain SH1 (Cys^{707}) and SH2 (Cys^{697}). Significantly less (10%, judging by eye) fluorescence was detected on a 25-kDa fragment containing the nucleotide-binding region. No fluorescence was detected on the 50-kDa fragment. Further evidence for the specificity of TMRIA for Cys^{707} came from ATPase assays: relative to unlabeled HMM, TMRIA-modified HMM showed a decreased rate of K^+-ATP hydrolysis, and an increased rate of Ca^{2+}-ATP hydrolysis, in proportion to the extent of labeling.

As mentioned above, Cys^{707} modification did affect the enzymatic activity of HMM. The physiologically relevant actin-activated Mg^{2+}-ATPase decreased slightly in proportion to the extent of TMRIA labeling, such that HMM labeled with two TMRIA per HMM hydrolyzed Mg^{2+}-ATP at 80% of the unmodified HMM rate.

Donor labeling

Donor chelate was placed on the light chain domain as follows. A solution of $TbCl_3$ was added at a 0.9:1 molar ratio to EMPH-DTPA-cs124 at pH 7 at millimolar concentration, and the metal was allowed to bind for 30 min on ice. A ~20-fold excess of the metal-containing chelate was then added to gizzard RLC in exchange buffer with 5 mM TCEP. The reaction was allowed to proceed for more than an hour (often overnight) at pH 7.0 on ice and quenched with 10 mM DTT. Gizzard RLC contains a unique cysteine (Cys^{108}, equivalent in position to Val^{103} on the skeletal RLC, based on sequence alignment; Collins, 1991).

Exchange reaction

Endogenous RLC was replaced with chelate-labeled gizzard RLC as follows. A 5- to 10-fold excess of Tb-gizzard RLC was added to HMM (either unlabeled or TMRIA-labeled) in exchange buffer, and the solution was heated to 34°C for 15 min, followed by cooling on ice and the addition of TES (pH 7.0) and then $MgCl_2$ to final concentrations of 100 mM and 15 mM (5 mM free Mg), respectively. Unincorporated RLC was eliminated, and the solvent changed, by passing over a G-75 column equilibrated in rigor buffer. Incorporation of gizzard RLC into skeletal HMM was confirmed by SDS-PAGE.

To check for nonspecific binding of the gizzard RLC to HMM, the two were mixed at concentrations identical to those used for exchange (5–8 μM HMM, 25–80 μM gizzard RLC). This mixture was left on ice for 15 min instead of being heated to 34°C, and then passed over a G75 column. No gizzard RLC was apparent on SDS-PAGE of this sample.

During the heating step of the exchange reaction, 1 mM ADP was required to preserve the enzymatic activity of the HMM (Setton and Muhlrad, 1984). In the presence of 1 mM ADP, both the K^+-ATPase and actin-activated Mg^{2+}-ATPase activities of HMM were unchanged after gizzard RLC exchange relative to untreated HMM.

Lanthanide luminescence measurements

All terbium emission data were recorded on a laboratory-built spectrophotometer described previously (Selvin and Hearst, 1994) and recently upgraded to include a CCD for spectral measurements (Selvin, 1996). Samples were placed in a quartz cuvette (either 3 mm × 3 mm or 2 mm × 2 mm inner dimensions) at room temperature. The concentration of HMM was typically 1 μM in rigor buffer. The concentration of actin, when present, was 4–10 μM. This actin concentration ensures complete binding of HMM (Greene, 1981). The terbium donor was excited with 400-1600 excitation pulses from a nitrogen laser (337 nm, 5-ns pulsewidth, 40-Hz repetition rate), and terbium emission (546 nm) was acquired after passing through a grating spectrometer with a photon-counting photomultiplier attached to a multichannel analyzer (2-μs resolution).

Curve-fitting and energy transfer analysis

Multiexponential fits were made with Tablecurve (Jandel Scientific, Marin, CA). Donor-only data were fit to two exponentials and showed no residual structure. Donor-acceptor data were fit to three exponentials and also showed no residual structure. The shortest lifetime (<90 μs) in the three-exponential fit was due to detector ringing arising from prompt acceptor emission immediately after the laser excitation pulse. It does not originate from luminescence of the terbium donor and hence is not included in the energy transfer analysis. The three-exponential fit of the donor-acceptor complex can be reduced to a two-exponential fit by fitting the data after a >150-μs delay, thereby eliminating the <90-μs component due to detector ringing. In the two-exponential fit, the shorter component (which is not of primary interest; see below) varied by 20% compared to the three-exponential fit, whereas the longer component, which is of primary interest, remained unchanged.

The efficiency of energy transfer was calculated from the lifetimes of donor luminescence as $1 - (\tau_{D/A}/\tau_D)$, where τ_D and $\tau_{D/A}$ are the donor excited state lifetimes in the absence and presence of acceptor, respectively. For each experiment, donor-only and donor-acceptor samples were prepared simultaneously, and all energy transfer calculations pair the

donor-acceptor measurement with the corresponding donor-only control. This pairwise method of comparison yielded highly reproducible results and is superior to determining energy transfer by comparing the average of donor-only lifetimes to the average of donor-acceptor lifetimes. A paired-sample *t*-test was used to determine the statistical significance of differences in energy transfer measurements between experimental conditions (HMM alone, HMM + actin, HMM + actin + ATP, HMM + actin + ADP). Throughout the text, lifetime and energy transfer data are reported as mean ± standard error of the mean.

Polarization measurements

Steady-state anisotropy measurements $[(I_{\parallel} - I_{\perp})/(I_{\parallel} + 2\,I_{\perp})]$ of TMRIA bound to myosin were performed according to standard methods using 514-nm vertically polarized excitation, a rotatable analyzer, and a second analyzer placed at 45° to eliminate detection polarization effects. In addition, an aperture was placed in the emission path to limit the numerical aperture, and a CCD was used as the detector (Selvin, 1996). Blank measurements on unlabeled myosin and unlabeled myosin bound to actin were subtracted from all signals. Measurements were performed at room temperature at ~0.5 μM TMRIA in a 3 mm × 3 mm cuvette.

Steady-state anisotropy measurements on the terbium-labeled gizzard RLC exchanged into HMM (without TMRIA) were performed similarly, except that excitation was with vertically polarized 337-nm pulsed light, and the emission was passed through a single analyzer and a chopper before being detected by the CCD. The polarization sensitivity of the optics was determined by assuming that the anisotropy of a Tb-DTPA-cs124 chelate freely diffusing in solution was zero. (The spectrometer had a 15.7% bias in favor of horizontally polarized light.)

RESULTS

Donor-only lifetime measurements

Fig. 1 shows the structure of the terbium chelate used as the donor. Except for the differences caused by the reactive maleimide group, the spectroscopic (Li and Selvin, 1995), structural (Selvin et al., 1996), and energy transfer properties of the chelate have been described (Selvin and Hearst, 1994; Selvin et al., 1994). The hydrazide-carbonyl linker used in the maleimide has the advantage that the carbonyl partially ligates the lanthanide, resulting in a higher lanthanide quantum yield and a longer excited-state lifetime than the equivalent complex without the hydrazide linkage (1.81 ms versus 1.55 ms, respectively; Li and Selvin, 1995). When bound to gizzard RLC and exchanged into HMM, the excited-state lifetime in the absence of acceptor is almost monoexponential, with 87 ± 1% of the signal decaying with a time constant of 1.81 ± 0.03 ms ($n = 5$) at room temperature (Table 1 and Fig. 2). In addition, there is a 13 ± 1% component decaying with a time constant of 0.57 ± 0.04 ms ($n = 5$). The source of this short lifetime component (4.3 ± 0.2% of the total photons) is unknown, but it indicates that a small population of the chelates (13%) have a quenched excited-state lifetime, possibly due to an altered interaction with the protein. The long lifetime, which is of primary interest, is highly reproducible, with a standard deviation of only 3% of the mean on five measurements on different days on different samples. Neither the short nor the long lifetime of the donor changes upon addition of actin or nucleotides. Specifically, binding of HMM to actin or nucleotide (ATP or ADP) causes a change in the short lifetime component of 0.05 ± 0.04 ms ($n = 7$), ~10% of the mean, and a change in the long lifetime component of only 0.005 ± 0.004 ms ($n = 7$), ~0.3% of the mean.

TABLE 1 Donor (Tb^{3+}) luminescent lifetime and energy transfer measurements on actomyosin

Sample (protein complex: labels)	Lifetime	Energy transfer (ET)	Δ in ET relative to HMM only
HMM: donor only	1.81 ± 0.03 ms ($n = 5$)	N/A	
HMM: donor-acceptor	1.42 ± 0.02 ms ($n = 5$)	21.2 ± 1.9% ($n = 5$)	
Acto-HMM: donor-acceptor	1.51 ± 0.04 ms ($n = 4$)	15.6 ± 2.6% ($n = 4$)	−4.5 ± 1.0% ($n = 4$)
ATP + acto-HMM: donor-acceptor	1.45 ± 0.05 ms ($n = 3$)	18.3 ± 3.0% ($n = 3$)	−1.4 ± 0.7% ($n = 3$)

For each experimental condition (column 1), the table lists the long lifetime component of donor luminescence (column 2), and the efficiency of energy transfer calculated by a pairwise comparison of the long lifetime components of donor emission from the donor-only and donor-acceptor complexes in each experiment (column 3). In the presence of acceptor, the donor's luminescent lifetime becomes shorter because of energy transfer between the terbium donor on the regulatory light chain and a TMRIA acceptor at Cys^{707} in the catalytic domain of HMM. Energy transfer efficiency is calculated as $1 - (\tau_{D/A}/\tau_D)$, where τ_D and $\tau_{D/A}$ are the lifetimes of donor luminescence in the absence and presence of acceptor, respectively. Note that energy transfer calculated by taking the ratio of the average lifetimes (from column 2) is not necessarily the same as energy transfer calculated pairwise for each experiment, then averaged (listed in column 3). (The pairwise method is more accurate.) A comparison of energy transfer in HMM alone to energy transfer measured in HMM after addition of saturating actin or actin + ATP is calculated pairwise for each experiment, and listed in column 4. Note that the change in energy transfer relative to the HMM-only sample must be calculated pairwise for each experiment, because the energy transfer values listed in column 3 are averages over different sample populations ($n = 5$ for HMM only, $n = 4$ for HMM + actin, $n = 3$ for HMM + actin + ATP). As indicated in column 4, binding of actin to HMM decreases energy transfer by an average of 4.5%, a small but statistically significant ($p < 0.01$) difference. Subsequent addition of ATP to acto-HMM returns energy transfer to within 1.4% of the HMM-only value, a difference that is not statistically significant ($p < 0.05$). All values are given as mean ± standard error of the mean.

Donor-acceptor lifetime measurements

When the chelate-labeled RLC is exchanged into an HMM labeled at Cys^{707} with acceptor, the decay of terbium emission at 546 nm is triexponential (Fig. 2). The shortest lifetime ($\tau < 0.09$ ms) in the three-exponential fit is due to detector ringing arising from prompt acceptor emission immediately after the laser excitation pulse. It has no physiological significance, and is not considered in the energy transfer analysis. The origin of the middle lifetime component ($\tau = 0.40–0.60$ ms) is more complex and is discussed in detail later (see Spectral Analysis). The lifetime of the longest component ($\tau = 1.40–1.60$ ms) is believed to be influenced by energy transfer between the terbium donor on the regulatory light chain and a TMRIA acceptor at Cys^{707}. An

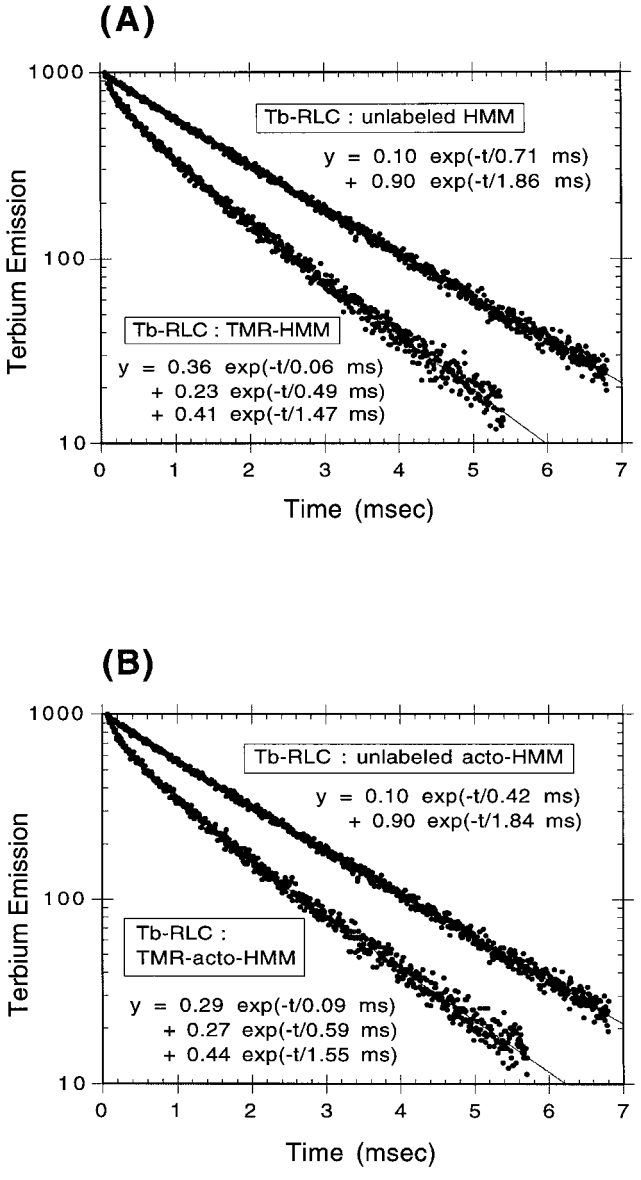

FIGURE 2 Excited-state lifetime of the terbium donor on HMM, with and without TMRIA acceptor. The terbium donor is placed on the regulatory light chain of HMM; the acceptor, if present, is placed at Cys^{707} in the catalytic domain of HMM. (*A*) A typical decay of terbium donor luminescence (emission measured at 546 nm after a 5-ns excitation pulse at 337 nm) in the absence and presence of acceptor for HMM without actin. The donor-only is nearly single exponential; the donor-acceptor is triexponential, although it is only the longest component that is of interest here (see text). The reduction of the long component of the terbium luminescent lifetime in the presence of acceptor indicates 21% energy transfer, or a distance of 73 Å. (*B*) The corresponding donor-only and donor-acceptor measurements after the addition of saturating actin to the HMM sample of *A*. Again, based on the reduction of the long-lifetime component, 15.8% energy transfer is inferred, indicating a conformational change upon addition of actin to HMM.

analysis of this component and the effect of adding actin, ATP, or ADP to HMM are presented here and in Table 1.

Comparing the donor's excited-state lifetime on HMM with and without acceptor (Table 1 and Fig. 2 *A*; no nucleotide or actin) yields 21.2 ± 1.9% energy transfer ($n = 5$), corresponding to a donor-acceptor distance of 73 Å (R_o = 59 Å; see below). A 2× dilution of the sample with buffer causes no change in the terbium lifetime, indicating that all energy transfer is intramolecular, and not intermolecular, as expected because of the dilute conditions and large molecular weight of HMM.

The addition of actin decreases the efficiency of energy transfer to 15.6 ± 2.6% ($n = 4$) (Table 1 and Fig. 2 *B*). A pairwise comparison of the HMM-only and HMM + actin measurements reveals a decrease in energy transfer upon actin binding of 4.5 ± 1.0% ($n = 4$). Note that although this difference is relatively small, it is statistically significant ($p < 0.01$) and highly reproducible.

We considered that the reduction in energy transfer observed upon actin binding could be due to decreased interaction between the two heads of an HMM molecule. To test this possibility, the single-headed myosin fragment, papain S1 (pS1), was prepared and labeled with TMRIA at Cys^{707} and exchanged with Tb-EMPH-labeled gizzard RLC, following the protocol outlined for HMM in Materials and Methods. Upon addition of actin to pS1 there was a decrease in energy transfer similar to the decrease observed in acto-HMM. These results indicate that the changes in energy transfer measured in HMM are not a result of energy transfer from a donor on the RLC of one head to an acceptor at Cys^{707} on the other head of the HMM dimer.

The addition of 1 mM ATP to acto-HMM, which at this ionic strength releases HMM almost entirely from actin (and starts the catalytic cycle), returns the efficiency of energy transfer to close to its HMM-only value, indicating that the myosin has been released from actin (see below for further discussion of this point). In Table 1, the small difference between the average amounts of energy transfer in the HMM-only and HMM + actin + ATP samples is actually a result of calculating the average over different sample populations ($n = 5$ for HMM only, $n = 3$ for HMM + actin + ATP). A pairwise comparison of the HMM-only and HMM + actin + ATP measurements reveals a difference in energy transfer of 1.4 ± 0.7% ($n = 3$), which is not statistically significant at the $p = 0.05$ confidence level.

In two separate experiments, the addition of 0.5 mM ADP to the actin-HMM complex caused a 3.4% increase in energy transfer. As discussed below, there is a body of evidence which indicates that TMRIA bound to Cys^{707} rotates upon the addition of actomyosin, whereas the global conformation of the myosin head does not change. Thus the observed change in energy transfer upon the addition of ADP is probably due primarily to a rotation of the rhodamine acceptor.

Spectral analysis

Components in spectra

As mentioned previously, the donor's excited-state lifetime is biexponential in both the donor-only and the donor-acceptor complex, but the relative population of the short component increases from 13 ± 1% to 31 ± 3% of all

chelates, respectively, with only a small change in the lifetime of this component ($\tau = 0.57 \pm 0.04$ ms in donor-only samples, 0.44 ± 0.04 ms in donor-acceptor samples). The increase in amplitude of the short component in the donor-acceptor samples indicates the presence of a second species of donor in addition to the quenched population seen in the donor-only samples. Thus the 31% component in the donor-acceptor samples, which has a (average) lifetime of 0.44 ms, arises from two distinct donor populations whose lifetimes cannot be resolved: 1) Thirteen percent arise from the chelates that are quenched even in the absence of acceptor. These donors have an excited lifetime of 0.57 ms. 2) Eighteen percent arise from donors that undergo a relatively large amount of energy transfer. These donors have a lifetime likely to be somewhat shorter than the 0.44-ms average, ~0.35 ms. This species of donor is relatively close to an acceptor—$1 - (0.35 \text{ ms}/1.81 \text{ ms}) = 81\%$ energy transfer, or 46 Å between donor and acceptor, based on an R_o of 59 Å (see below). This short-lived component contributes to sensitized emission (data not shown), which is strong evidence that it is indeed arising from energy transfer. The fraction of terbium emission that decays with this shorter lifetime does not change upon binding of HMM to actin or nucleotides. The source of this 18% population is unknown, although it may be due to acceptor labeling at a site other than Cys^{707}, or to an altered conformation of the protein.

Calculation of R_o

The distance measured in resonance energy transfer experiments is inferred using the well-known equation $E = 1/[1 + (R/R_o)^6]$, or $R = R_o(1/E - 1)^{1/6}$ (Cantor and Schimmel, 1980). R_o is defined by the equation $R_o = (8.79 \times 10^{-5} J\kappa^2 n^{-4} q_D)^{1/6}$ Å, where parameters appropriate to lanthanide photophysics are used (Selvin, 1996; Selvin and Hearst, 1994). Specifically, q_D is the lanthanide quantum yield in the absence of acceptor, J is the spectral overlap of the donor's electric dipole emission (f_D) and acceptor absorption (ϵ_A) ($J = \int f_D \epsilon_A \lambda^4 \, d\lambda$), n is the index of refraction, and κ^2 is a geometric factor related to the relative angles of the two dipoles. R_o has previously been evaluated for Tb to TMRIA (Selvin and Hearst, 1994). Using the parameters appropriate for myosin (see below), we find that $R_o = 59$ Å.

Here we discuss each term in R_o and discuss its uncertainty. We use $\epsilon_{554nm} = 69 \text{ mM}^{-1} \text{ cm}^{-1}$ and $\epsilon_{280nm} = 0.29\epsilon_{554nm}$. Others have measured ϵ_{554nm} to be $47 \text{ mM}^{-1} \text{ cm}^{-1}$ (DeBiasio et al., 1988) and 79 mM (Ajtai et al., 1992); the former would reduce R_o by 5% (to 56 Å), and the latter would increase R_o by 3% (to 61 Å). We set $q_D = 0.7 = 1.81$ ms/2.63 ms, the latter corresponding to the lifetime in D_2O (Li and Selvin, 1995), where q_D is assumed to be unity in D_2O (Selvin and Hearst, 1994). We also assume that terbium emission in the 546-nm manifold is due only to electric dipole transitions. This is clearly an upper limit for q_D and for the fraction of electric dipole emission (as opposed to magnetic dipole transitions, which cannot transfer energy), but these assumptions yield reasonable distances in model systems (Selvin and Hearst, 1994; Selvin et al., 1994). We use $n = 1.33$ (the value for water); if we were to use $n = 1.39$, the value for many organic materials, R_o, would be reduced by 3%. Although these parameters affect the absolute distance calculated, they do not significantly affect the difference in distance we find between the myosin-only and the myosin-actin complex.

The last term, κ^2, is typically the most problematic, although dos Remedios has argued that even in conventional FRET measurements on actomyosin, assuming that $\kappa^2 = 2/3$ yields reliable results (dos Remedios and Moens, 1995). With terbium as a donor, emission is unpolarized (anisotropy of 546 nm emission = 0.039), which is equivalent to a rapidly rotating donor. This constrains $1/3 < \kappa^2 < 4/3$, the limits corresponding to an acceptor that is completely rigid and aligned perpendicular or parallel, respectively, to the radius vector. Assuming $\kappa^2 = 2/3$ then produces at most a 12% error in R_o if the acceptor is completely rigid (Dale et al., 1979). We measured an anisotropy of 0.34 for TMRIA bound to myosin at Cys^{707} and a value of 0.33 upon addition of actin, in good agreement with previous measurements (Ajtai et al., 1992). These measurements indicate that the TMRIA is quite rigid on the nanosecond time scale (0.34 corresponds to a wobble in a cone of half-angle 26°, assuming the dye's dipole moment is equally distributed within the wobble cone before it emits, and that the maximum anisotropy is 0.40), limiting the error in R_o due to orientation to approximately ±10%. Furthermore, in LRET, rotational motion of the acceptor during the donor's millisecond lifetime will further constrain κ^2 near 2/3. Long-lifetime protein breathing motions are known to occur on this time scale (Wells and Yount, 1982).

Nevertheless, the changes in energy transfer seen upon the addition of actin or ADP are relatively small, on the order of 5%. Consequently, changes in the orientation of the acceptor could generate these changes in energy transfer, and as discussed below, the observed changes are probably influenced by rotation and possibly distance changes.

DISCUSSION

The present investigation represents the first application of LRET to the determination of distances in actomyosin. A primary result is that, although the distance between Cys^{707} and the light chain domain is large, it can be determined by LRET, and the result agrees with the crystal structure of myosin subfragment-1. In the absence of nucleotide, we find the distance from Cys^{707} in the catalytic domain to Cys^{108} in the regulatory light chain domain to be 73 Å, in good agreement with a 68-Å C_α-to-C_α distance from Cys^{707} to Val^{103} in the crystal structure of Rayment et al. The largest source of uncertainty in our measured distance is the estimation of R_o: the uncertainty in the orientation factor leads to an uncertainty in distance of ±10%, and the lanthanide quantum yield assumption (see previous discussion of R_o) may lead to an overestimation of the actual distance,

although this error is probably significantly smaller than that due to the orientation factor. In addition, the distance we measure is not necessarily comparable to that of the crystal structure. Aside from the obvious solution-versus-crystalline conditions, our distance includes the effects of side chains, dye linkers, and the finite size of the dyes, and is measured from Cys^{108} of the gizzard light chain, whereas in the crystal it is from Val^{103} of the native skeletal light chain. The dyes and linkers together are on the order of 7–10 Å.

Interpretation of the small changes in energy transfer that occur upon addition of actin or nucleotides must consider alterations in both the distance and the orientation of the acceptor. The addition of actin to HMM decreases the efficiency of energy transfer, showing that there has been a change in the conformation of HMM between Cys^{707} and the light chain. This change could reflect either a rotation of the acceptor bound at Cys^{707} or an increase in distance between donor and acceptor. If the change in energy transfer is due to a pure translation, the distance in the acto-HMM complex would be 78.7 Å, a 4.2-Å increase over the HMM-only distance. However, conformational changes upon actin binding are known to occur in the vicinity local to Cys^{707}, as shown by dye reactivity measurements, suggesting that rotation of the acceptor could contribute to changes in LRET (Ando, 1984; Duke et al., 1976; Kameyama, 1980).

The addition of ADP to acto-HMM increases the energy transfer by 3.4% relative to the acto-HMM complex. This is likely due to a rotation of the TMRIA acceptor bound to Cys^{707}. There is evidence that the angle of tetramethylrhodamine bound to Cys^{707} changes by at least 20–30° upon binding of ADP to rigor fibers (Burghardt et al., 1983; Tanner et al., 1992). Because the angle between the rhodamine dipole moment and the radius vector is not known, this rotation could account for the increase in energy transfer we detect upon addition of ADP to acto-HMM. In addition, there is reasonable evidence that under these conditions the global conformation of skeletal myosin does not change with the addition of ADP to actomyosin, indicating that at least large-scale distance changes between the light chain domain and the catalytic domain probably do not occur. Specifically, there is no appreciable change in the angles of paramagnetic or fluorescent probes bound to the light chains in skeletal muscle fibers (Allen et al., 1996; Gollub et al., 1996; Hambly et al., 1991). It thus appears that the change in energy transfer upon the addition of ADP to acto-HMM likely reflects a change in acceptor orientation, although a change in distance may play a small role.

The addition of ATP to acto-HMM also changes the energy transfer, back to its myosin-only value. Under the conditions used, the addition of ATP releases HMM almost entirely from actin. However, the interpretation of this result in terms of myosin conformation is difficult for a number of reasons: 1) ATP starts the catalytic cycle and hence produces a distribution of myosin states, and 2) labeling at Cys^{707} likely alters the mechanical properties and relative populations of myosin states during active cycling (Marriott and Heidecker, 1996; Root and Reisler, 1992; Sleep et al., 1981).

CONCLUSION

We have shown that LRET is capable of measuring distances between the catalytic and light chain domains of myosin, and that the result is consistent with the crystal structure of the myosin head. Energy transfer decreases a small but significant amount upon addition of actin, and returns to near its myosin-only value with the further addition of ADP. Hence these substrates cause a conformational change in myosin—probably a rotation in the Cys^{707} region, and possibly a small relative translation between Cys^{707} and the light chain domain as well. These measurements demonstrate the feasibility of using LRET for more detailed studies of actomyosin during the many states of its catalytic cycle.

We thank Christine Cremo for the gift of gizzard regulatory light chain and Kathy Franks-Skiba for help with protein preparation.

This work was supported by a Bank of America–Giannini Foundation Fellowship (EBG), and by National Institutes of Health grants AR44420 (PRS) and AR42895 (RC) and by the Office of Energy Research, Office of Health and Environmental Research of the Department of Energy, under contract DE AC03-76SF00098 (PRS).

REFERENCES

Ajtai, K., P. J. K. Ilich, A. Ringler, S. S. Sedarous, D. J. Toft, and T. P. Burghardt. 1992. Stereospecific reaction of muscle fiber proteins with the 5′ and 6′ isomer of (iodoacetamido)tetramethylrhodamine. *Biochemistry.* 31:12431–12440.

Allen, T. S. C., N. Ling, M. Irving, and Y. E. Goldman. 1996. Orientation changes in myosin regulatory light chains following photorelease of ATP in skinned muscle fibers. *Biophys. J.* 70:1847–1862.

Ando, T. 1984. Fluorescence of fluorescein attached to myosin SH1 distinguishes the rigor state from the actin-myosin-nucleotide state. *Biochemistry.* 23:375–381.

Burghardt, T. P., T. Ando, and J. Borejdo. 1983. Evidence for cross-bridge order in contraction of glycerinated skeletal muscle. *Proc. Natl. Acad. Sci. USA.* 80:7515–7519.

Cantor, C. R., and P. R. Schimmel. 1980. Biophysical Chemistry. W. H. Freeman and Co., San Francisco.

Collins, J. H. 1991. Myosin light chains and troponin C: structural and evolutionary relationships revealed by amino acid sequence comparisons. *J. Muscle Res. Cell Motil.* 12:3–25.

Cooke, R. 1997. Actomyosin interaction in striated muscle. *Physiol. Rev.* 77:671–697.

Dale, R. E., J. Eisinger, and W. E. Blumberg. 1979. The orientational freedom of molecular probes. *Biophys. J.* 26:161–194.

DeBiasio, R. L., L.-L. Wang, G. W. Fisher, and D. L. Taylor. 1988. The dynamic distribution of fluorescent analogues of actin and myosin in protrusions at the leading edge of migrating Swiss 3T3 fibroblasts. *J. Cell Biol.* 107:2631–2645.

dos Remedios, C. G., M. Miki, and J. A. Barden. 1987. Fluorescence resonance energy transfer measurements of distances in actin and myosin. A critical evaluation. *J. Muscle Res. Cell Motil.* 8:97–117.

dos Remedios, C. G., and P. D. J. Moens. 1995. Fluorescence resonance energy transfer spectroscopy is a reliable "ruler" for measuring structural changes in proteins. *J. Struct. Biol.* 115:175–185.

Duke, J., R. Takashi, K. Ue, and M. F. Morales. 1976. Reciprocal reactivities of specific thiols when actin binds to myosin. *Proc. Natl. Acad. Sci. USA.* 73:302–306.

Finer, J. T., R. M. Simmons, and J. A. Spudich. 1994. Single myosin molecule mechanics: piconewton forces and nanometre steps. *Nature.* 368:113–119.

Fisher, A. J., C. A. Smith, J. B. Thoden, R. Smith, K. Sutoh, H. M. Holden, and I. Rayment. 1995. X-ray structures of the myosin motor domain of *Dictyostelium discoideum* complexed with MgADP·BeF_x and MgADP·AlF_4^-. *Biochemistry.* 34:8960–8972.

Gollub, J., C. R. Cremo, and R. Cooke. 1996. ADP release produces a rotation of the neck region of smooth myosin but not skeletal myosin. *Nature Struct. Biol.* 3:796–802.

Greene, L. 1981. Comparison of the binding of heavy meromyosin and myosin subfragment 1 to F-actin. *Biochemistry.* 20:2120–2126.

Hambly, B., K. Franks, and R. Cooke. 1991. Orientation of spin-labeled light chain-2 exchanged onto myosin cross-bridges in glycerinated muscle fibers. *Biophys. J.* 59:127–138.

Hambly, B., K. Franks, and R. Cooke. 1992. Paramagnetic probes attached to a light chain on the myosin head are highly disordered in active muscle fibers. *Biophys. J.* 63:1306–1313.

Heyduk, E., T. Heyduk, P. Claus, and J. R. Wisniewski. 1997. Conformational changes of DNA induced by binding of chironomus high mobility group protein 1a (cHMG1a). *J. Biol. Chem.* 272:19763–19770.

Horrocks, W. D., Jr., B. Holmquist, and B. L. Vallee. 1975. Energy transfer between terbium(III) and cobalt(II) in thermolysins: a new class of metal-metal distance probes. *Proc. Natl. Acad. Sci. USA.* 72: 4764–4768.

Huxley, H. E. 1965. The mechanism of muscular contraction. *Sci. Am.* 213:18–27.

Irving, M., T. S. Allen, C. Sabido-David, J. S. Craik, B. Brandmeier, J. Kendrickjones, J. E. T. Corrie, D. R. Trentham, and Y. E. Goldman. 1995. Tilting of the light-chain region of myosin during step length changes and active force generation in skeletal muscle. *Nature.* 375: 688–691.

Jontes, J. D., E. M. Wilsonkubalek, and R. A. Milligan. 1995. A 32-degrees tail swing in brush border myosin I on ADP release. *Nature.* 378: 751–753.

Kameyama, T. 1980. Actin-induced local conformational change in the myosin molecule. II. Conformational change around the S2 thiol group related to the essential intermediate of ATP hydrolysis. *J. Biochem.* 87:581–586.

Kodama, T., K. Fukui, and K. Kometani. 1986. The initial phosphate burst in ATP hydrolysis by myosin and subfragment-1 as studied by a modified malachite green method for determination of inorganic phosphate. *J. Biochem.* 99:1465–1472.

Li, M., and P. R. Selvin. 1995. Luminescent lanthanide polyaminocarboxylate chelates: the effect of chelate structure. *J. Am. Chem. Soc.* 117: 8132–8138.

Li, M., and P. R. Selvin. 1997. Amine-reactive forms of a luminescent DTPA chelate of terbium and europium: attachment to DNA and energy transfer measurements. *Bioconjug. Chem.* 8:127–132.

Marriott, G., and M. Heidecker. 1996. Light-directed generation of the actin-activated ATPase activity of caged heavy meromyosin. *Biochemistry.* 35:3170–3174.

Mathis, G. 1993. Rare earth cryptates and homogeneous fluoroimmunoassays with human sera. *Clin. Chem.* 39:1953–1959.

Mathis, G. 1995. Probing molecular interactions with homogeneous techniques based on rare earth cryptates and fluorescence energy transfer. *Clin. Chem.* 41:1391–1397.

Mendelson, R. A., D. K. Schneider, and D. B. Stone. 1996. Conformations of myosin subfragment-1 ATPse intermediates from neutron and x-ray scattering. *J. Mol. Biol.* 256:1–7.

Rayment, I., H. M. Holden, M. Whittaker, C. B. Yohn, M. Lorenz, K. C. Holmes, and R. A. Milligan. 1993a. Structure of the actin-myosin complex and its implications for muscle contraction. *Science.* 261: 58–65.

Rayment, I., W. R. Rypniewski, K. Schmidt-Base, R. Smith, D. R. Tomchick, M. M. Benning, D. A. Winkelmann, G. Wesenberg, and H. M. Holden. 1993b. Three-dimensional structure of myosin subfragment-1: a molecular motor. *Science.* 261:50–57.

Root, D. D. 1997. In situ molecular association of dystrophin with actin revealed by sensitized emission immuno-resonance energy transfer. *Proc. Natl. Acad. Sci. USA.* 94:5685–5690.

Root, D. D., and E. Reisler. 1992. Cooperativity of thiol-modified myosin filaments: ATPase and motility assays of myosin function. *Biophys. J.* 63:730–740.

Schröder, R. R., D. J. Manstein, W. Jahn, H. Holden, I. Rayment, K. C. Holmes, and J. A. Spudich. 1993. Three-dimensional atomic model of F-actin decorated with *Dictyostelium* myosin S1. *Nature.* 364:171–174.

Selvin, P. R. 1995. Fluorescence resonance energy transfer. *Methods Enzymol.* 246:300–334.

Selvin, P. R. 1996. Lanthanide-based resonance energy transfer. *IEEE J. Selected Top. Quantum Electron. Lasers in Biol.* 2:1077–1087.

Selvin, P. R., and J. E. Hearst. 1994. Luminescence energy transfer using a terbium chelate: improvements on fluorescence energy transfer. *Proc. Natl. Acad. Sci. USA.* 91:10024–10028.

Selvin, P. R., J. Jancarik, M. Li, and L.-W. Hung. 1996. Crystal structure and spectroscopic characterization of a luminescent europium chelate. *Inorg. Chem.* 35:700–705.

Selvin, P. R., T. M. Rana, and J. E. Hearst. 1994. Luminescence resonance energy transfer. *J. Am. Chem. Soc.* 116:6029–6030.

Setton, A., and A. Muhlrad. 1984. Effect of mild heat treatment on the ATPase activity and proteolytic sensitivity of myosin subfragment-1. *Arch. Biochem. Biophys.* 235:411–417.

Sleep, D. R., K. M. Trybus, K. A. Johnson, and E. W. Taylor. 1981. Kinetic studies of normal and modified heavy meromyosin and subfragment-1. *J. Muscle Res. Cell Motil.* 2:373–399.

Smith, C. A., and I. Rayment. 1995. X-ray structure of the magnesium(II)-pyrophosphate complex of the truncated head of *Dictyostelium discoideum* myosin to 2.7 Å resolution. *Biochemistry.* 34:8973–8981.

Smith, C. A., and I. Rayment. 1996. X-ray structure of the magnesium(II). ADP·vanadate complex of the *Dictyostelium discoideum* myosin motor domain to 1.9 Å resolution. *Biochemistry.* 35:5404–5417.

Smyczynski, C., and A. A. Kasprzak. 1997. Effect of nucleotides and actin on the orientation of the light chain-binding domain in myosin subfragment 1. *Biochemistry.* 36:13201–13207.

Spudich, J. A. 1994. How molecular motors work. *Nature.* 372:515–518.

Spudich, J. A., and S. Watt. 1971. The regulation of rabbit skeletal muscle contraction. I. Biochemical studies of the interaction of the tropomyosin-troponin complex with actin and the proteolytic fragments of myosin. *J. Biol. Chem.* 246:4866–4871.

Stryer, L., D. D. Thomas, and C. F. Meares. 1982. Diffusion-enhanced fluorescence energy transfer. *Annu. Rev. Biophys. Bioeng.* 11:203–222.

Tanner, J. W., D. D. Thomas, and Y. E. Goldman. 1992. Transients in orientation of a fluorescent cross-bridge probe following photolysis of caged nucleotides in skeletal muscle fibres. *J. Mol. Biol.* 223:185–203.

Uyeda, T. Q., P. D. Abramson, and J. A. Spudich. 1996. The neck region of the myosin motor domain acts as a lever arm to generate movement. *Proc. Natl Acad. Sci. USA.* 93:4459–4464.

Wakabayshi, K., I. Tokunaga, O. Y. Kohn, T. Sugimoto, T. Hamanaka, Y. Takezawa, T. Wakabayshi, and Y. Amemiya. 1992. Small angle synchrotron x-ray scattering reveals distinct shape changes of the myosin head during hydrolysis of ATP. *Science.* 258:443–447.

Weeds, A. G., and B. Pope. 1977. Studies of the chymotryptic digestion of myosin. Effects of divalent cations on proteolytic susceptibility. *J. Mol. Biol.* 111:129–157.

Wells, J. A., and R. G. Yount. 1982. Chemical modification of myosin by active site trapping of metal-nucleotides with thiol cross-linking reagents. *Methods Enzymol.* 85:93–116.